

INTRINSIC DEGENERACY OF GRAVITATIONAL LENS TIME DELAYS: THE CASE FOR A SIMPLE QUADRUPLE SYSTEM IN Λ CDM COSMOLOGY

HONGSHENG ZHAO AND BO QIN^{1,2}
To be published in ApJ, 582, 000 (2003)

ABSTRACT

A degeneracy in strong lens model is shown analytically. The observed time delays and quasar image positions might *not* uniquely determine the concentration and the extent of the lens galaxy halo mass distribution. Simply hardwiring the Hubble constant (H_0) and the cosmology (Ω, Λ) to the standard Λ CDM cosmology values might *not* fully lift this degeneracy, which exists rigorously even with very accurate data. Equally good fits to the images could be found in lens mass models with either a mostly Keplerian or a flat rotation curve. This degeneracy in mass models makes the task of getting reliable H_0 and Λ from strong lenses even more daunting.

Subject headings: cosmological parameters—dark matter—distance scale —gravitational lensing

1. INTRODUCTION

One of the promises of gravitational lenses is to measure the Hubble constant H_0 (Refsdal 1964) from the observed time delays among the images of a variable background quasar source lensed by a foreground galaxy. Given a model for the spatial distributions of the stars and dark matter in the lens galaxy, the time delay Δt_{obs} multiplied by the speed of light c is simply proportional to the absolute distances to the lens and the source, hence $c\Delta t_{\text{obs}}$ scales with the size of the universe c/H_0 . While the time delays are now routinely measured for many systems (see Schechter 2000), a reliable determination of H_0 has been hampered to some extent by the intrinsic degeneracy in models of the dark matter potential of the lens (Williams & Saha 2000; Saha 2000; Zhao & Pronk 2001). The general trend is that a model with a dense dark matter halo gives a small H_0 with

$$H_0 \Delta t_{\text{obs}} \propto [2\Sigma_{\text{crit}}(z_l, z_s) - \Sigma_*(R_E) - \Sigma_h(R_E)], \quad (1)$$

where $\Sigma_{\text{crit}}(z_l, z_s)$ is the critical density for the lens at redshift z_l and the source at z_s , and $\Sigma_*(R_E)$ or $\Sigma_h(R_E)$ is the typical surface density of luminous or dark matter at within the Einstein ring R_E (Falco, Gorenstein, & Shapiro 1985; Kochanek 2002).

Given that the value of H_0 is now well constrained by other independent methods, such as the HST Key Project (Freedman et al. 2001), it is interesting to reverse the angle of the question, and use equation (1) to put more stringent constraint on the dark matter potential of the lens. More specifically in this *Letter*, we would like to ask the question: how narrow is the allowed parameter space for the lens dark halo which is consistent with a given set of images, time delays, cosmology and H_0 ? In the interest of clarity, we will consider only analytical lens models with a simplified geometry for a hypothetical image and lens system. We believe our arguments should apply qualitatively to real galaxy lenses as well, and a more detailed application to the quadruple system PG1115+080 is given in a follow-up paper (Zhao & Qin 2002).

2. ANALYTICAL LENS MODELS FOR STARS AND HALO

For simplicity we assume the four images form a perfectly symmetric Einstein cross with the time delay minima on the y-axis at $\pm R_E$ (radian) from the lens center, and the saddle point images on the x-axis at $\pm q R_E$ (radian). For generality we rescale the images, taking the radius R_E as unity in a new XY coordinate system, so the four images are given by

$$[X, Y]_{\text{minima}} = [0, \pm 1], \quad [X, Y]_{\text{saddle}} = [\pm q, 0]. \quad (2)$$

This image configuration implies that a source $(X_s, Y_s) = (0, 0)$, exactly behind a spherical lens plus a linear external shear symmetric to the X and Y axes.

All lensing properties can be derived from the time delay surfaces. For our model with spherical stellar lens $\phi_*(R)$ plus halo $\phi_h(R)$ and a linear shear of amplitude γ_1 , the time delay contours are determined by a dimensionless time delay $\tau(X, Y)$ given by

$$\begin{aligned} \tau(X, Y) &= t \cdot \omega(H_0, \Omega, z_l, z_s) R_E^{-2} \\ &= \frac{X^2 + Y^2}{2} - \frac{\gamma_1(X^2 - Y^2)}{2} - \phi_*(R) - \phi_h(R) \end{aligned} \quad (3)$$

where $R = \sqrt{X^2 + Y^2}$ is the cylindrical radius, and $\omega(H_0, \Omega, z_l, z_s)$ is a constant containing all the dependence on the cosmological density parameter Ω and the lens and source redshifts z_l, z_s ; crudely speaking $\omega \sim H_0$ for typical lens and source redshifts in the Λ CDM cosmology.

To illustrate the non-uniqueness, we need to find reasonable lens models with similar time delay surface. Let's consider the following example of lensing potential for the stars,

$$\phi_*(R) = \frac{m_0}{\alpha} \ln \left(1 + \frac{R^\alpha}{a^\alpha} \right) \quad (5)$$

where m_0 is the total stellar mass enclosed, a is the half mass radius, and $2 - \alpha$ specifies the cuspleness of the stellar distribution. For the halo we use a nearly isothermal potential

$$\phi_h(R) = b_0 R^{-\frac{\delta}{2}} [(1, R^2)_{\text{min}} + \ln(1, R^2)_{\text{max}} + \ln^2(1, R^2)_{\text{max}}] \quad (6)$$

¹ National Astronomical Observatories, Chinese Academy of Science, Beijing 100012, PRC

² Institute of Astronomy, Madingley Road, Cambridge, CB3 0HA, U.K. (zhao,qinbo@ast.cam.ac.uk)

where $\sqrt{b_0}$ is proportional to the terminal velocity of the halo rotation curve.

Note that the function ϕ_h is smoothly connected at the two sides of the radius $R = 1$, which is chosen such that it is just outside the images. The parameter δ is a dimensionless tunable parameter to adjust the halo contribution to the surface density at $R = 1$. The surface density can be computed as

$$\kappa(R) = 1 - \frac{1}{2}\nabla^2\tau, \quad (7)$$

so the densities for the stars and the halo are given by

$$\kappa_*(R) = \frac{\alpha m_0 a^\alpha}{2R^{2-\alpha}(R^\alpha + a^\alpha)^2}, \quad \kappa_h(R) = \frac{b_0}{2R} - \frac{\delta}{[1, R^2]_{\max}}. \quad (8)$$

Note that the stars have an inner cusp $2 - \alpha$, and the halo density κ_h is continuous across the break $R = 1$, and positive everywhere if $b_0/\delta > 2$.

By increasing δ we can lower the mean densities at the images, hence creating the effect of a negative mass sheet. This will not affect the positions of the images, but can increase the time delay $\Delta\tau_{\text{obs}} \propto H_0\Delta t_{\text{obs}}$ between the images. As we will see, this can result in a larger H_0 to be consistent with the currently favored high value of $H_0 \sim 70 \text{ km s}^{-1} \text{ Mpc}^{-1}$.

The deflection strength

$$b(R) \equiv \frac{d\phi}{dR} \equiv \frac{M_*(< R) + M_h(< R)}{R} \quad (9)$$

is effectively the rotation curve squared. A flat rotation curve corresponds to a constant deflection strength. For our model, the stellar and halo masses enclosed inside radius R are given by

$$M_* = \frac{m_0 R^\alpha}{R^\alpha + a^\alpha}, \quad M_h = b_0 R - \delta [(1, R^2)_{\min} + \ln(1, R^2)_{\max}]. \quad (10)$$

As we can see the stars converge to a finite mass m_0 at infinity and the halo dominates stars and approaches to a finite deflection (terminal velocity $\propto \sqrt{b_0}$).

3. RESULTS

Let's consider a typical lensing system in a standard Λ CDM cosmology with

$$H_0 = 70 \text{ km s}^{-1} \text{ Mpc}^{-1}, \quad \Omega = 1 - \Lambda = 0.3 \quad (11)$$

with the lens and source redshifts

$$z_l = 0.5, \quad z_s = 2, \quad (12)$$

and a time delay Δt_{obs}

$$(t_{\text{saddle}}^{\text{obs}} - t_{\text{mimima}}^{\text{obs}}) = 28 \text{ day} \left[\left(\frac{R_E}{1''} \right)^2 - \left(\frac{qR_E}{1''} \right)^2 \right], \quad q = 0.5 \quad (13)$$

between the saddle point image at $(qR_E, 0)$ and the minima image at $(0, R_E)$.

The above cosmology specifies the distances to the lens and the source, hence the time delay normalization constant

$$\omega(H_0 = 70, \Omega = 1 - \Lambda = 0.3, z_l = 0.5, z_s = 2) \sim 100 \text{ km s}^{-1} \text{ Mpc}^{-1} \quad (14)$$

The observed time delay then set the following constraint on the lens model,

$$\Delta\tau_{\text{obs}} = \tau(0.5, 0) - \tau(0, 1) \quad (15)$$

$$= \frac{(t_{\text{saddle}}^{\text{obs}} - t_{\text{mimima}}^{\text{obs}})}{R_E^2} \omega \quad (16)$$

$$\sim 28(1 - q^2) \text{ day}/\square'' \times 100 \text{ km s}^{-1} \text{ Mpc}^{-1} \sim 0.22 \quad (17)$$

We solve for the parameters of the lens and the shear to reproduce the four images at $(\pm q, 0)$, $(0, \pm 1)$ exactly. The images form at the extreme points of the time delay surface, hence we have the additional constraints

$$\frac{\partial\tau}{\partial X} = 0, \quad \frac{\partial\tau}{\partial Y} = 0, \quad \text{at } (X, Y) = (0.5, 0) \text{ and } (0, 1). \quad (18)$$

It turns out that the allowed models follow a three-parameter sequence, say (δ, a, α) . The parameters of a few representative models are listed in Table 1. The images appear rigorously at the same locations for all four models, which are the minima and saddle points of the arrival time surfaces (cf. Figure 1a), and the relative time delay is identical as well for all four lens models (cf. Figure 1b). But the mass distributions in the four models are far from similar (cf. Figure 2a and Figure 2b): lensIII and lensIV correspond to systems with a finite stellar core with a very typical half-mass radius R_e about half of the Einstein radius R_E ; lensIV is purely in stars, and has no halo. Both lensI and lensII correspond to systems with a strong stellar cusp dominating the halo at small radii; lensII has a bigger stellar component with a half-mass radius at one R_E .

3.1. The cause of degeneracy

The above degeneracy is a variation of the well-known mass-sheet degeneracy. The latter implies that we can increase H_0 by reducing the surface density $\kappa = \frac{\Sigma}{2\Sigma_{\text{crit}}}$ at the Einstein radius R_E (cf. equation (1)), e.g., by either scaling down the stellar mass m_0 or scaling down the isothermal dark halo mass $b_0 r$. But if we reduce the stellar mass m_0 and increase the halo mass $b_0 r$ *simultaneously* such that we keep $\kappa_*(R_E) + \kappa_h(R_E)$ constant (between 0.10 to 0.13, cf. Table 1), then $H_0\Delta t_{\text{obs}}$ will not change, only the terminal velocity of the rotation curve $\sqrt{b_0}$ is raised. The result is a rigorous degeneracy of the stellar vs. halo mass distribution, insensitive to H_0 and the observed time delay Δt_{obs} .

3.2. Break the degeneracy from observable flux ratio and lens light profile?

The flux ratio of the saddle image and the minima image can in principle differentiate some of the models, as shown by Fig. 3. But assuming a reasonable ± 0.1 mag error with the magnitude, and a 10% error with the effective radius, most of the models are in fact degenerate. In particular, it will be difficult to constrain the mass of the stellar component m_0 .

Observations of a well-resolved stellar lens can fix the effective radius $a = R_e/R_E$ and perhaps the cuspsness $2 - \alpha$. This reduces the available lens models drastically. Nonetheless, the degeneracy between lensIII and lensIV implies that it is still problematic to differentiate between models with dark halo and models without. To break the

degeneracy one needs at least an accurate measurement of the external shear γ_1 to 10% level (cf. the parameters of lensIII and lensIV in Table 1), perhaps by a combination of strong lensing and weak lensing data.

4. CONCLUSION AND COMPARISON WITH EARLIER MODELS

It is possible to construct many very different models with positive, smooth and monotonic surface densities to fit the image positions. There are also no extra images. These models fit the same images, time delay, H_0 and cosmology. Some fit the same lens light profile and image flux ratio as well. Hence the models are virtually *indistinguishable* from lensing data. There are severe degeneracies in inverting the data of a perfect Einstein cross to the lens models, even if given the Hubble constant and cosmology. These rigorous findings with analytical models are also consistent with earlier numerical models of Saha & Williams (2001) and semi-analytical models of Zhao & Pronk (2001).

Among the acceptable models the rotation curve can be Keplerian or flat (Fig. 2a), so lensing data plus H_0 cannot uniquely specify the lens mass profile. Among models in the literature, isothermal models and other simple smooth models of dark matter halos of gravitational lenses often

predict a dimensionless time delay $H_0 \Delta t_{\text{obs}}$ much too small (e.g., Schechter et al. 1997) to be comfortable with the observed time delays Δt_{obs} and the widely accepted value of $H_0 \sim 70 \text{ km s}^{-1} \text{ Mpc}^{-1}$. Naively speaking the high H_0 suggests a strangely small halo as compact as the stellar light distribution (Kochanek 2002). But our analytical models suggest that there are still many other options. The high H_0 implies that κ is small $\sim 0.1 - 0.2$ at the images, but this does not necessarily imply a rapidly falling density. A high H_0 does not necessarily mean no dark halo, and models with a flat rotation curve does not always yield a small H_0 (e.g., compare lensIII and lensIV in Figure 2b, both satisfy $h_0 = 0.7$). We also comment that it will be difficult to determine the cosmology from strong lensing data alone because the non-uniqueness in the lens models implies that the combined parameter $\omega(H_0, \Omega, z_l, z_s)$ is poorly constrained by the lensing data, even if H_0, z_l and z_s are given.

We thank the referee P. Saha for insightful comments on the cause of the degeneracy. This work was supported by the National Science Foundation of China under Grant No. 10003002 and a PPARC rolling grant to Cambridge. HSZ and BQ thank the Chinese Academy of Sciences and the Royal Society respectively for a visiting fellowship, and the host institutes for local hospitalities during their visits.

REFERENCES

- Falco, E.E., Gorenstein, M.V., & Shapiro, I.I., 1985, ApJ, 289, L1
 Freedman, W.L., Madore, B.F., Gibson, B.K., et al., 2001, ApJ, 553, 47
 Kochanek, C., 2002, ApJ, submitted (astro-ph/0205319)
 Refsdal, S., 1964, MNRAS, 128, 307
 Saha, P., 2000, AJ, 120, 1654
 Schechter, P.L., et al., 1997, ApJ, 475, L85
 Schechter, P.L., 2000, IAU 201, Lasenby, A.N., & Wilkinson, A., eds. (astro-ph/0009048)
 Williams, L.L.R., & Saha, P., 2000, AJ, 119, 439
 Saha, P., & Williams L.L.R., 2001, AJ, 122, 585
 Zhao, H.S., & Pronk, D., 2001, MNRAS, 320, 401
 Zhao, H.S., & Qin, B., 2002, ApJ, submitted (Paper II)

TABLE 1

PLAUSIBLE LENS PARAMETERS TO FIT THE IMAGES OF A PERFECT EINSTEIN CROSS AND TIME DELAYS WITH $H_0 = 100h_0 = 70 \text{ km s}^{-1} \text{ Mpc}^{-1}$ (CF. EQUATIONS (15) AND (18)).

| Model | Stars $\frac{M_0}{R_E^2}$ | Half-mass $a = \frac{R_c}{R_E}$ | Cusp $2 - \alpha$ | Halo $\frac{b_0}{R_E}$ | δ | Shear γ_1 | Conv. $\kappa_*(R_E)$ | $\kappa_h(R_E)$ | Mass $\frac{M_*(\leq R_E)}{R_E^2}$ | $\frac{M_h(\leq R_E)}{R_E^2}$ |
|---------|------------------------------|------------------------------------|----------------------|---------------------------|----------|---------------------|--------------------------|-----------------|---------------------------------------|-------------------------------|
| lensI | .2002 | .5 | 1. | .6220 | .2 | -.4445 | .0222 | .1110 | .1334 | .4220 |
| lensII | .7110 | 1. | 1. | .2988 | .1 | -.4458 | .0888 | .0494 | .3555 | .1988 |
| lensIII | .4901 | .5 | 0. | .2759 | .1 | -.4317 | .0784 | .0379 | .3921 | .1759 |
| lensIV | .7129 | .5 | 0. | .0013 | 0. | -.4291 | .1140 | .0006 | .5703 | .0013 |

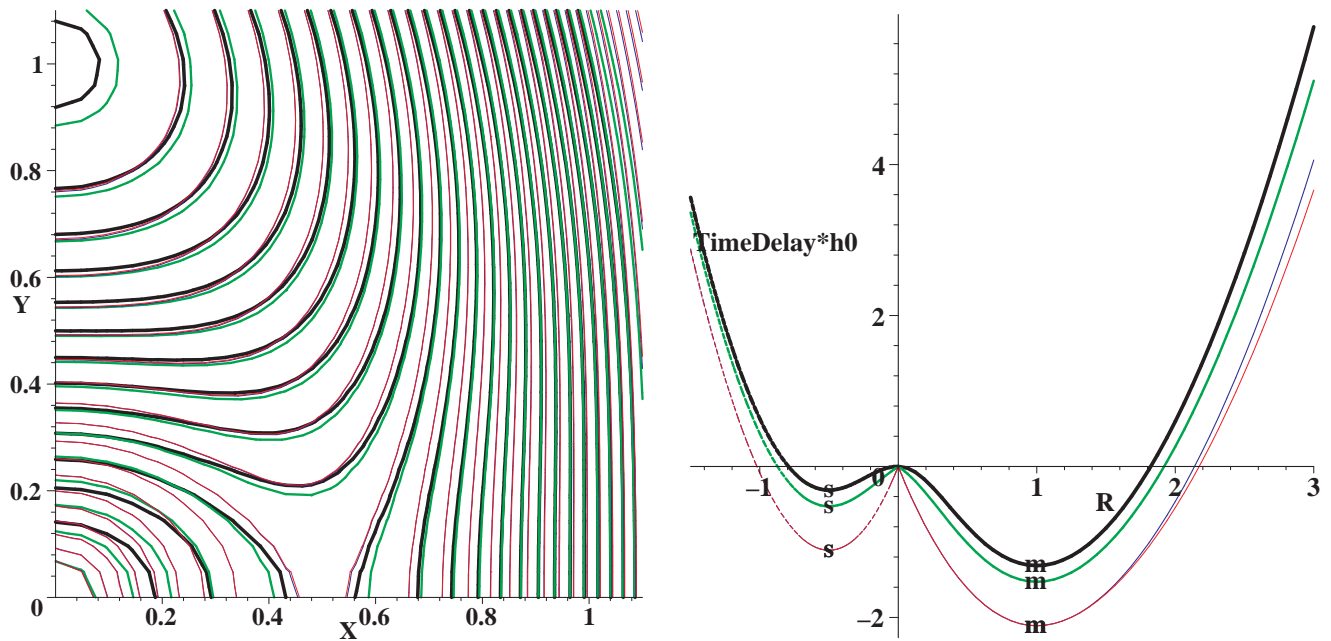


FIG. 1.— Panel (a): Time delay contours in the XY quadrant in intervals of 3 days for the four lens models. All models reproduce the same minima and saddle image positions and time delay. Panel (b): Cuts of the time delay surfaces $\frac{t(R)}{(t_{\text{saddle}}^{\text{obs}} - t_{\text{minima}}^{\text{obs}})h_0^{-1}}$ as a function of the radius R along the radial direction from the lens to the time delay minima (marked by “m” on solid curves to the right) and from the lens to the saddle image (marked by “s” on dashed curves to the negative R side) for all four lens models. All models use $h_0 = 0.7$ and the same time delay between the images “s” and “m”.

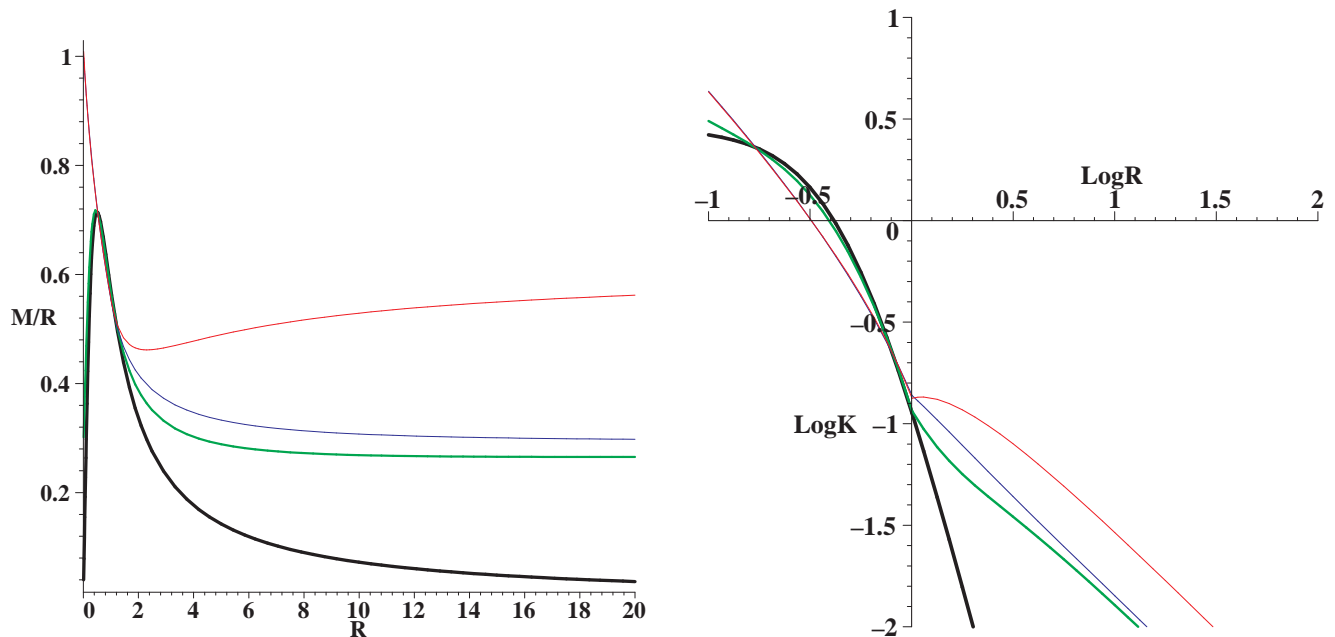


FIG. 2.— Panel (a): The deflection strength of the lens $b = M(R)/R$ as a function of distance from the lens; this is effectively a rotation curve of the lens. From top right to down right, from thinner to thicker lines, the models are color coded as red (lens I), blue (lens II), green (lens III) and black (lens IV). Both Keplerian and flat rotation curve models are found. Panel (b): Log-Log plot of the surface density profiles $\kappa(R)$ of the four lens models. All models have very low κ at the images near $-0.3 \leq \log R \leq 0$, consistent with a high H_0 . In all models except for lens IV (black), stars are dominated by dark matter halos just beyond the Einstein radius at $\log R \sim 0$.

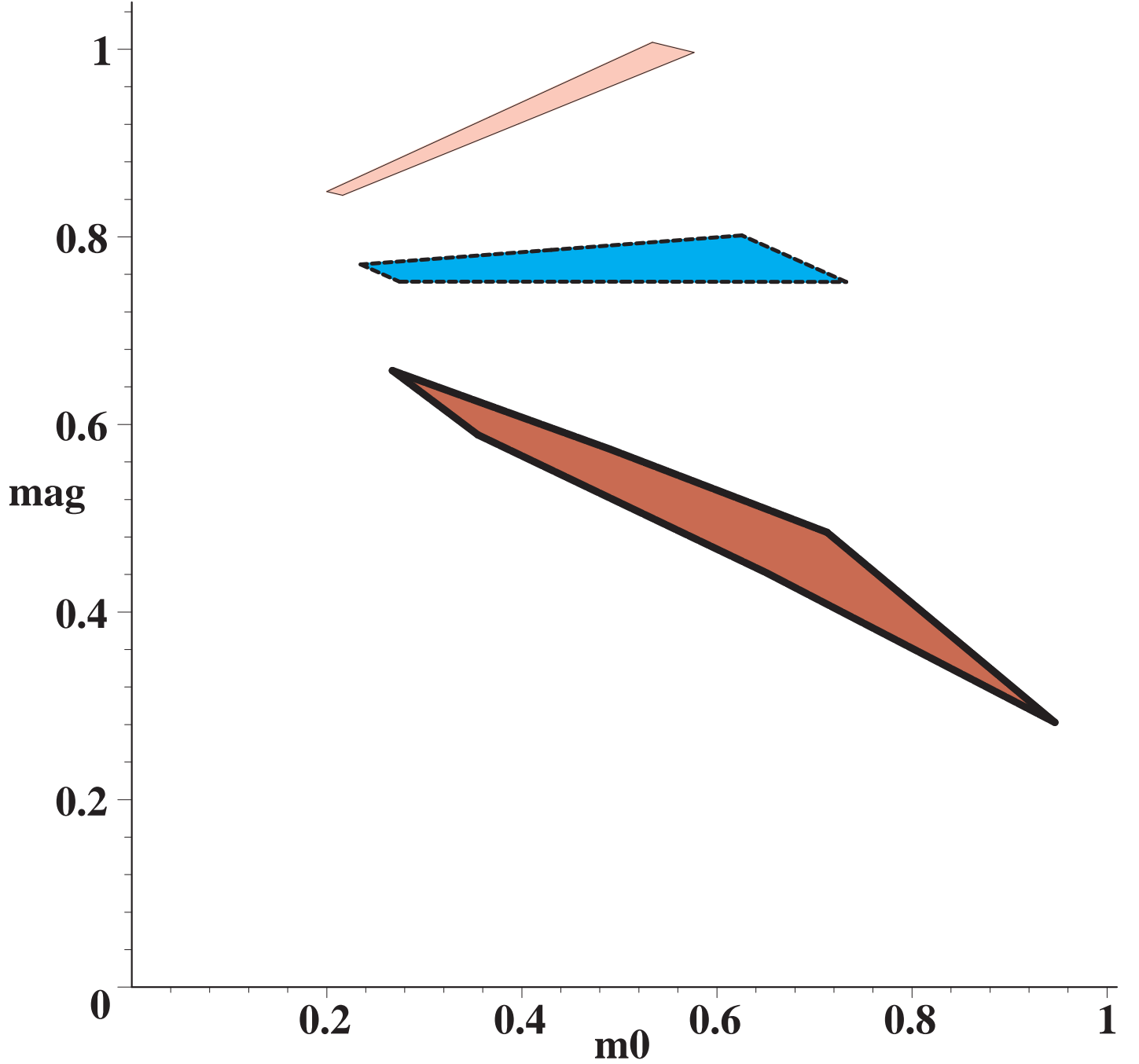


FIG. 3.— The relative magnitude of images as a function of stellar mass of the model m_0 . From top to down (color coded as pink, cyan and orange) the painted polygons correspond to stellar cusps of slope $2 - \alpha = 1, 0.5, 0$. Clockwise from the rightmost corner the four corners of each polygon correspond to $[\delta, a] = [0, 0.55], [0.2, 0.55], [0.2, 0.5], [0, 0.5]$. If these models are extended to $\delta = 0.3$, then all models merger to a point on the vertical axis, i.e., a pure-halo model with $m_0 \sim 0$.